Downloaded from orbit.dtu.dk on: Oct 10, 2024

DTU Library

A Multi-Time Scale Energy Management Method for Active Distribution Networks with Multiple Terminal Soft Open Point

Sun, Fengzhou; Yu, Miao; Wu, Qiuwei; Wei, Wei

Published in:
International Journal of Electrical Power & Energy Systems

Link to article, DOI:
10.1016/j.ijepes.2021.106767

Publication date:
2021

Document Version
Peer reviewed version

Link back to DTU Orbit

Citation (APA):
Sun, F., Yu, M., Wu, Q., & Wei, W. (2021). A Multi-Time Scale Energy Management Method for Active Distribution Networks with Multiple Terminal Soft Open Point. *International Journal of Electrical Power & Energy Systems*, *128*, Article 106767. https://doi.org/10.1016/j.ijepes.2021.106767

General rights
Copyright and moral rights for the publications made accessible in the public portal are retained by the authors and/or other copyright owners and it is a condition of accessing publications that users recognise and abide by the legal requirements associated with these rights.

- Users may download and print one copy of any publication from the public portal for the purpose of private study or research.
- You may not further distribute the material or use it for any profit-making activity or commercial gain
- You may freely distribute the URL identifying the publication in the public portal

If you believe that this document breaches copyright please contact us providing details, and we will remove access to the work immediately and investigate your claim.

A Multi-Time Scale Energy Management Method for Active Distribution Networks with Multiple Terminal Soft Open Point

Fengzhou Sun, Miao Yu, Qiuwei Wu, and Wei Wei

Highlights

- A multi-time scale energy management framework is proposed to improve the economic efficiency, security and robustness of the active distribution network jointly.
- The economic benefits of the active distribution network and multiple independent microgrids can be well balanced by the day-ahead Stackelberg game model.
- The voltage deviation can be remarkably reduced at small economic cost by the proposed day-ahead reactive power optimization model.
- V^2-P and V^2-Q droop control is implemented in the multiple terminal soft open point to absorb the intraday power fluctuations and convex the proposed intraday robust model.
- A branch loss limit strategy is proposed in the subproblem of the intraday model to improve the accuracy of the second-order cone relaxation.

A B S T R A C T-- This paper proposed a multi-time scale robust energy management method for active distribution networks with the multiple terminal soft open point where the active distribution network and microgrids belonged to different ownerships. In the day-ahead Stackelberg game model, the time-of-use price and active power exchange plan between the active distribution network and microgrids were optimized under power flow constraints to balance economic benefits of all participants. Then a reactive power re-optimization model was established to minimize system voltage deviation under the tolerant cost constraint by utilizing residual capacity of voltage source converters. In the intraday model, considering the fluctuations of actual power exchange of microgrids, V^2-P and V^2-Q droop control mode was implemented in the soft open point, and a slope robust optimization model was established to improve system robust security within the uncertainty set. Case studies show that the proposed method can efficiently utilize the flexible power flow regulation capability of the multiple terminal soft open point, and improve both economic benefits and reliability of the system.

Keywords: droop control, multiple terminal soft open point, robust optimization, Stackelberg game.

NOMENCLATURE

Sets

B	Set of buses.
E	Set of branches.
$B_{\text{sop,S}}$	Set of buses connected to the slave terminals of the SOP.
$B_{\text{sop,M}}$	Set of buses connected to the master terminal of the SOP.
U	Set of RES uncertainty.
K^l	Set of extreme scenarios in the l^{th} iteration.
D	Set of expected scenarios.

Parameters

n	The number of day-ahead dispatch periods.
Δt	The time interval of each period.
z_1	The number of relaxed buses connected to the main grid.
z_2	The number of controllable DGs.
z_3	The number of MGs.
z_4	The number of terminals of the SOP.
C_{e}^t	Time-of-use electricity buying price of the ADN (from the main grid) at time t.
$C_{\text{d,base}}$	Unit generation cost of controllable DGs.
$C_{\text{d,p}}$	Unit penalty cost of controllable DGs.
r_{ij} / x_{ij}	Resistance/reactance of branch ij.
b_j	Shunt susceptance from bus j to the ground.
$S_{\text{sop,max}}$	Rated apparent power of the SOP terminal.
$S_{\text{vsc,max},m}$	Rated apparent power of the m^{th} VSC.
w_{wt}, w_{pv}	Operating cost coefficients of WT and PV.
w_{es}	Operating cost coefficients of ES.
P_{load}^t	The internal load of the MG at time t.
S_{CAP}	The ES capacity.
soc_{max}	The maximum state of charge of ES.
soc_{min}	The minimum state of charge of ES.
soc_s	The initial state of charge of ES.
$P_{\text{in,max}}$	The maximum charge power of ES.
$P_{\text{out,max}}$	The maximum discharge power of ES.
$P_{\text{pv,f}}^t$, $P_{\text{wt,f}}^t$	Day-ahead forecast output power of PV and WT.
V_{max}, V_{min}	Upper/lower limit of voltage magnitude.
I_{max}	Upper/lower limit of current magnitude.

Variables

$P_{\text{e},m}^t$	The injection power from the m^{th} relaxed bus at time t.

This work was supported by National Natural Science Foundation of China (U1909201). (*Corresponding author: Miao Yu.*)

Fengzhou Sun, Miao Yu and Wei Wei are with College of Electrical Engineering, Zhejiang University, Hangzhou, China. (E-mail: sunfz@zju.edu.cn, zjuyumiao@zju.edu.cn, wwei@zju.edu.cn).

Qiuwei Wu is with the Center for Electric Power and Energy, Department of Electrical Engineering, Technical University of Denmark, Elektrovej 325, Kgs. Lyngby, Denmark 2800 (qw@elektro.dtu.dk).

$P_{\mathrm{d},m}^{t}$ The output power of the m^{th} controllable DG at time t.

$P_{\mathrm{b},m}^{t}$ Power of the m^{th} MG bought from the ADN at time t.

$P_{\mathrm{s},m}^{t}$ Power of the m^{th} MG sold to the ADN at time t.

$C_{\mathrm{b},m}^{t}$ Time-of-use buying price of the m^{th} MG at time t.

$C_{\mathrm{s},m}^{t}$ Time-of-use selling price of the m^{th} MG at time t.

V_{i}^{t} Voltage magnitude of bus i at time t.

I_{ij}^{t} Current magnitude of branch ij at time t.

P_{ij}^{t} Active power flow from bus i to j at time t.

Q_{ij}^{t} Reactive power flow from bus i to j at time t.

$P_{\mathrm{inj},i}^{t}$ Active power injection at bus i at time t.

$Q_{\mathrm{inj},i}^{t}$ Reactive power injection at bus i at time t.

$P_{\mathrm{sop},m}^{t}$ Active power of the m^{th} SOP terminal at time t.

$Q_{\mathrm{sop},m}^{t}$ Reactive power of the m^{th} SOP terminal at time t.

$P_{\mathrm{vsc},m}^{t}$ Active power of the m^{th} VSC at time t.

$Q_{\mathrm{vsc},m}^{t}$ Reactive power of the m^{th} VSC at time t.

$P_{\mathrm{wt}}^{t}, P_{\mathrm{pv}}^{t}$ Output power of WT and PV at time t.

$P_{\mathrm{in}}^{t}, P_{\mathrm{out}}^{t}$ Charging and discharging power of ES at time t.

soc^{t} The state of charge of ES at time t.

$k_{\mathrm{p},i}, k_{\mathrm{q},i}$ Active and reactive droop slopes.

1. Introduction

Nowadays, with the rapid development of renewable energy sources (RESs), the combination of the active distribution network (ADN) and multiple microgrids (MGs) is an effective way to achieve flexible connections to diverse kinds of power sources and loads [1]. Under this background, the newly emerging flexible interconnection technology based on soft open points (SOPs) can provide additional degrees of control freedom to the system operation [2]. The SOP is a novel power electronic device which enables the flexible connection between different feeders or subgrids [3]. It is conducive to realizing flexible power flow regulation, alleviating line congestion and improving the renewable energy absorption ability [4].

In the ADN with the SOP, how to design a reasonable interactive mechanism and realize coordinated operation between the ADN and MGs is the key issue for the security and economy of the system, and the SOP can be fully utilized to adjust power flow and regulate system voltage. A coordinated SOP voltage regulation method is proposed in [5] to decrease the probability of the voltage violation. In [6], a multi-agent system based model predictive control method is proposed in the real-time power dispatch to compensate the power control error of MGs. In [7], a generic power injection model is developed using the Powell's direct set method to determine the optimal SOP operation point so that the network loss can be minimized. However, the researches mentioned above all consider the system as a unified stakeholder with one single objective.

In practical situation, the ADN and MGs connected to it may belong to different stakeholders, and multiple conflicting objectives need to be considered simultaneously [8]. The market-based price-driven energy management framework has been proven to be an effective way to deal with this issue. The studies can mainly be classified into two groups, i.e., peer-to-peer structure and leader-follower structure. The peer-to-peer structure is suitable for the energy exchange among equal subjects within the community under loose management policy [9]. A fair energy sharing framework is proposed in [10] for a community of energy buildings to achieve the largest cost reductions and ensure the fairness of the cost reduction ratios for each building. In [11], a localized event-driven market model is built to facilitate indirect customer-to-customer energy trading. The energy trading process is modeled as a Markov decision process with the reinforcement learning method. When there is a leader acting as the retailer or the price maker, the leader-follower structure is more effective to coordinate the interests of different stakeholders. A two-stage energy sharing management method for the prosumer microgrid is proposed in [12]. In the first stage, the retailer and prosumers reach an agreement on the internal price and energy sharing plan based on the Stackelberg game. While in the second stage, the energy sharing plan is updated in real time considering the RES output power deviation. A priority-based MG energy management framework is proposed in [13] by layering different MGs according to their importance. The lexicographic optimization method is applied to solve the proposed model. However, the above researches all assume that most local participants are geographically close to each other and connected to the same distribution feeder. Therefore, the power flow constraints of the distribution network are ignored.

Note that when the retailer is the ADN itself, the ADN needs to consider not only the operation cost but also the power flow security and voltage quality. Therefore, additional restrictions should be added on the trading plans. A decentralized Stackelberg game algorithm with non-converging penalties is proposed in [14] to conduct the negotiations among different objectives of networked MG clusters. In [15], a multi-objective optimal reactive power dispatch model solved by the weighting method is proposed to achieve trade-offs between power system's optimal operational performance and the minimal number of control adjustments. But the weights of objectives with different dimensions are difficult to determine. An improved tolerant lexicographic optimization model is proposed in [16] to solve the multi-objective system reconfiguration model aiming to minimize a set of reliability indices and obtain the Pareto front. In the above researches, the dispatch performance highly depends on the accuracy of the forecast data. How to absorb or suppress the intraday RES uncertainty and adjust the dispatch plan adaptively to guarantee system security is also an important issue for the market-based energy management [17].

To cope with RES power uncertainty, robust optimization is widely adopted in many researches, which can guarantee a reliable dispatch in the presence of RESs' uncertain output power [18]. A two-level interactive robust model is proposed in [19] to address the day-ahead scheduling of the ADN with MG clusters. The distributed iteration method is used to solve the model. However, the convergence of the algorithm and the Nash equilibrium cannot be guaranteed under the time-of-use price mechanism. The

incentive and guidance effect of time-of-use price for MGs needs to be further improved. In [20], a two-stage adjustable robust optimization method is proposed to achieve the robust optimal operation of SOPs in the ADN under the worst scenario, which may lead to over-conservative results. In [21], the operation cost of MG clusters is minimized under the expected scenarios while ensuring the system security within the uncertainty set to improve the conservatism of the robust model. However, the grid structure and power flow security constraints are ignored, which makes the proposed method unsuitable for the ADN [22]. In order to make the power flow equation of distribution systems compatible to the robust optimization model, second-order cone (SOC) relaxation based branch flow model is proposed in [23] and solved by the column-and-constraint generation (CCG) algorithm, which decomposes the original model into a master problem and a sub-problem. But there is usually large inaccuracy of the SOC relaxation in this method. To mitigate the effects of the relaxation, a cutting plane iteration method is proposed in the master problem [24]. However, inaccuracy of the SOC relaxation still exists in the subproblem, which may affect the reliability of the optimization results and need to be further studied.

To solve the aforementioned problems, this paper proposes a multi-time scale robust energy management method for the ADN with the multiple terminal SOP. The main contributions of this paper are summarized as follows:

1) In the day-ahead dispatch, a Stackelberg game model considering power flow constraints is established to balance economic benefits between the ADN and MGs belonging to different ownerships. The time-of-use electricity price and active power exchange plan between the ADN and MGs are optimized.

2) A reactive power re-optimization model is established to fully utilize the residual capacity of voltage source converters (VSCs) to decrease system voltage deviation with the tolerant cost constraint, while the MG internal dispatch schedule is not affected.

3) In the intraday dispatch, considering the uncertainty and fluctuations of actual power exchange of MGs, a slope optimization model for $V^2 - P$ and $V^2 - Q$ dual droop control is established to improve system robust security based on day-ahead optimization results. An improved branch loss limit strategy is proposed to strengthen the accuracy of the SOC relaxation.

2. Energy management framework

The typical configuration of an ADN with the multiple terminal SOP is shown in Fig. 1. The AC/DC converter is adopted in each terminal of the SOP, and the control strategy can be set independently. The ADN contains controllable distributed generations (DGs), ADN owned load and MGs. Multiple MGs are connected to the ADN at different buses through MG owned VSCs, which can realize bi-directional power interaction. Each MG consists of MG owned load, the wind turbine (WT), photovoltaic system (PV) and energy storage (ES). The overall framework of the proposed energy management method can be divided into the day-ahead dispatch stage and the intraday dispatch stage, as shown in Fig. 2.

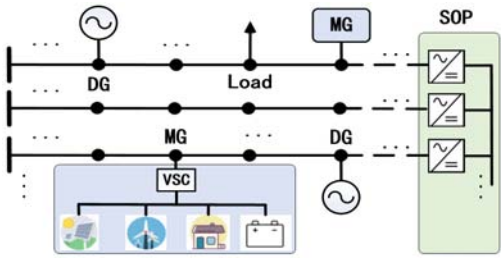

Fig. 1. The typical configuration of an ADN with the SOP.

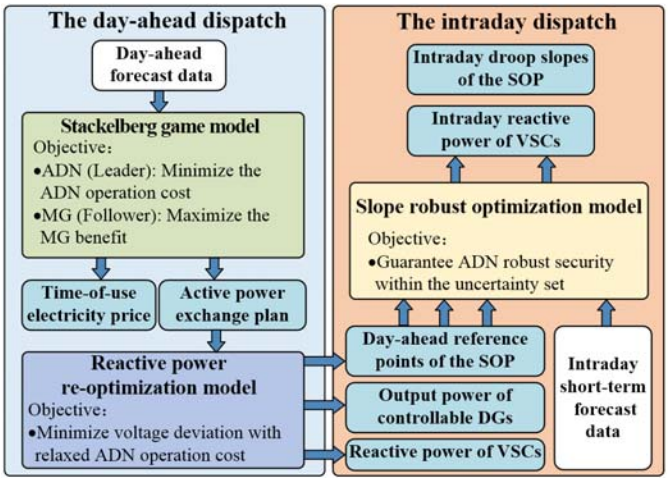

Fig. 2. The overall framework of the proposed energy management method.

2.1. Day-ahead scheduling strategy

In this paper, the ADN and MGs belong to different stakeholders. For the ADN, both economic efficiency and voltage safety margin need to be considered under power flow security constraints [25]. Therefore, the day-ahead dispatch model is decomposed into a Stackelberg active-reactive power co-optimization game model and a reactive power optimization model. In the Stackelberg game model, to balance the economic benefits of the ADN and MGs, the time-of-use buying and selling price mechanism is adopted for the bi-directional active power exchange between the ADN and each MG. As a leader, the ADN sets separate time-of-use prices for different MGs and formulates scheduling schemes for ADN owned devices to minimize the operating cost. As a follower, each MG formulates the internal scheduling scheme and the electricity exchange plan according to the time-of-use price to maximize its own benefit. In the reactive power optimization model, the VSC residual reactive capacity is re-dispatched to make a trade-off between economic efficiency and voltage safety margin of the ADN with the tolerant cost constraint, through which the Pareto front can be obtained and the decision makers of the ADN can quantitatively determine how much economic cost they are willing to bear in exchange for the improvement of voltage deviation.

It should be noted that, according to the capacity cost allocation method [26], reactive power compensation cost can be divided into explicit cost and opportunity cost. When VSC active power is fixed and VSC loss is neglected, both explicit cost and opportunity cost are zero. Therefore, to guarantee the benefit of MGs, it is reasonable to assume that the residual capacity of VSCs can be fully dispatched by the ADN after the time-of-use price and active power exchange are determined.

2.2. Intraday scheduling strategy

Due to the uncertainty of RESs, in the intraday dispatch stage, the actual output power of RESs may deviate from the forecast data, resulting in power imbalance in MGs. The power imbalance can be suppressed by the secondary scheduling of MGs, or absorbed by the ADN [27]. This paper mainly focuses on the secure and efficient ADN operation and the power imbalance is considered to be completely absorbed by the ADN. To solve this issue, V^2-P and V^2-Q dual droop control are implemented in the multiple terminal SOP. Then, based on the day-ahead optimization results and short-term forecast data, the robust optimization model of droop parameters is established to minimize the total network losses of the ADN under expected scenarios while ensuring the system robust security. Note that minimizing network losses is equivalent to minimizing the controllable operating cost of the ADN in the intraday dispatch stage.

3. Day-ahead Stackelberg game model

The day-ahead Stackelberg game model consists of the ADN leader model and the MG follower model, which are expressed below.

3.1. Active distribution network model

In the co-optimization model, the objective of the ADN shown in (1) is to minimize the operation cost by setting an independent time-of-use price for each MG and formulating scheduling schemes for ADN owned devices.

$$L=\min\sum_{t=1}^{n}\left[\begin{array}{l}\sum_{m=1}^{z_1}C_{\mathrm{e}}^{t}P_{\mathrm{e},m}^{t}+\sum_{m=1}^{z_2}(C_{\mathrm{d,base}}+C_{\mathrm{d,p}})P_{\mathrm{d},m}^{t}\\+\sum_{m=1}^{z_3}(C_{\mathrm{s},m}^{t}P_{\mathrm{s},m}^{t}-C_{\mathrm{b},m}^{t}P_{\mathrm{b},m}^{t})\end{array}\right]\Delta t \tag{1}$$

As shown in (1), the operation cost of the ADN consists of four parts: the cost of buying electricity from main grid, the cost of generating electricity from controllable DGs, the cost of buying electricity from MGs and the revenue of selling electricity to MGs. Note that $C_{\mathrm{d,p}}$ is extra penalty cost of controllable DGs. The purpose of setting the penalty cost is to encourage power exchange between the ADN and MGs, and controllable DGs can only be activated when system security is endangered.

The AC branch flow constraints are as follows [23],

$$P_{\mathrm{inj},j}^{t}+\sum_{j:i\to j}(P_{ij}^{t}-r_{ij}\tilde{I}_{ij}^{t})=\sum_{k:j\to k}P_{jk}^{t},\forall t,\forall j\in B \tag{2}$$

$$Q_{\mathrm{inj},j}^{t}+\sum_{j:i\to j}(Q_{ij}^{t}-x_{ij}\tilde{I}_{ij}^{t})+b_j\tilde{V}_{j}^{t}=\sum_{k:j\to k}Q_{jk}^{t},\forall t,\forall j\in B \tag{3}$$

$$\tilde{V}_{j}^{t}=\tilde{V}_{i}^{t}-2(r_{ij}P_{ij}^{t}+x_{ij}Q_{ij}^{t})+(r_{ij}^{2}+x_{ij}^{2})\tilde{I}_{ij}^{t},\forall t,\forall(i,j)\in E \tag{4}$$

$$P_{ij}^{t\,2}+Q_{ij}^{t\,2}=\tilde{I}_{ij}^{t}\tilde{V}_{i}^{t},\forall t,\forall(i,j)\in E \tag{5}$$

$$\tilde{I}_{ij}^{t}=I_{ij}^{t\,2},\forall t,\forall(i,j)\in E \tag{6}$$

$$\tilde{V}_{j}^{t}=V_{j}^{t\,2},\forall t,\forall j\in B \tag{7}$$

Constraints (2)-(3) represent the active and reactive power balance of bus j, respectively. Constraints (4) represents the Ohm's law of branch ij. The current magnitude of branch ij is determined by power formula (5).

Then, the quadratic equality (5) can be further relaxed into the following SOC inequality,

$$\left\|\begin{array}{c}2P_{ij}^{t}\\2Q_{ij}^{t}\\\tilde{I}_{ij}^{t}-\tilde{V}_{i}^{t}\end{array}\right\|_2\le\tilde{I}_{ij}^{t}+\tilde{V}_{i}^{t},\forall t,\forall(i,j)\in E \tag{8}$$

The security constraints of the ADN are,

$$V_{\min}^{2}\le\tilde{V}_{j}^{t}\le V_{\max}^{2},\forall t,\forall j\in B \tag{9}$$

$$0\le\tilde{I}_{ij}^{t}\le I_{\max}^{2},\forall t,\forall(i,j)\in E \tag{10}$$

Constraint (9) represents the system voltage limit. Constraint (10) represents the system current limit.

The constraints of the multiple terminal SOP and the VSCs are,

$$\sum_{m=1}^{z_4}P_{\mathrm{sop},m}^{t}=0,\forall t \tag{11}$$

$$P_{\mathrm{sop},m}^{t\,2}+Q_{\mathrm{sop},m}^{t\,2}\le S_{\mathrm{sop,max}}^{2},\forall t,\forall m \tag{12}$$

$$P_{\mathrm{vsc},m}^{t\,2}+Q_{\mathrm{vsc},m}^{t\,2}\le S_{\mathrm{vsc,max},m}^{2},\forall t,\forall m \tag{13}$$

$$P_{\mathrm{b},m}^{t}+P_{\mathrm{s},m}^{t}=P_{\mathrm{vsc},m}^{t},\forall t,\forall m \tag{14}$$

Constraint (11) represents the power balance equality of the SOP. The capacity constraints of the SOP and VSCs are expressed as (12) and (13).

The price constraints are,

$$(1-\beta)C_{\mathrm{f}}^{t}\le C_{\mathrm{b},m}^{t}\le(1+\beta)C_{\mathrm{f}}^{t},\forall t,\forall m \tag{15}$$

$$(1-\beta)C_{\mathrm{f}}^{t}\le C_{\mathrm{s},m}^{t}\le(1+\beta)C_{\mathrm{f}}^{t},\forall t,\forall m \tag{16}$$

$$C_{\mathrm{s},m}^{t}\le\alpha C_{\mathrm{b},m}^{t},\forall t,\forall m \tag{17}$$

where β and α are price coefficients between 0 and 1. As shown in (15)-(16), the ADN can independently determine the time-of-use buying and selling price of each MG within a certain range based on the time-of-use price of the main grid. Constraint (17) prevents MGs from buying and selling electricity at the same time to obtain arbitrage.

3.2. Microgrid model

The operation cost of an MG consists of five parts: the operation cost of PV, WT and ES, the cost of buying electricity from the ADN and the revenue of selling electricity to the ADN. Taking the m^{th} MG as an example, the objective function is shown in (18) (Subscript m is omitted below).

$$\max\sum_{t=1}^{n}\left[\begin{array}{l}C_{\mathrm{s}}^{t}P_{\mathrm{s}}^{t}-C_{\mathrm{b}}^{t}P_{\mathrm{b}}^{t}-w_{\mathrm{wt}}P_{\mathrm{wt}}^{t}\\-w_{\mathrm{pv}}P_{\mathrm{pv}}^{t}-w_{\mathrm{es}}(P_{\mathrm{in}}^{t}+P_{\mathrm{out}}^{t})\end{array}\right]\Delta t \tag{18}$$

The power balance constraints are,

$$P_{\mathrm{pv}}^{t}+P_{\mathrm{wt}}^{t}+P_{\mathrm{out}}^{t}+P_{\mathrm{b}}^{t}=P_{\mathrm{in}}^{t}+P_{\mathrm{s}}^{t}+P_{\mathrm{load}}^{t},\forall t \tag{19}$$

The ES constraints are,

$$\mathrm{soc}^{t+1} = \mathrm{soc}^{t}(1-\sigma) + \frac{\eta P_{\mathrm{in}}^{t}\Delta t}{S_{\mathrm{CAP}}} - \frac{P_{\mathrm{out}}^{t}\Delta t}{\eta S_{\mathrm{CAP}}}, \forall t \tag{20}$$

$$\mathrm{soc}^{1} = \mathrm{soc}^{n+1} = \mathrm{soc}_{s} \tag{21}$$

$$\mathrm{soc}_{\min} \le \mathrm{soc}^{t} \le \mathrm{soc}_{\max}, \forall t \tag{22}$$

$$0 \le P_{\mathrm{in}}^{t} \le P_{\mathrm{in,max}}, \forall t \tag{23}$$

$$0 \le P_{\mathrm{out}}^{t} \le P_{\mathrm{out,max}}, \forall t \tag{24}$$

where σ and η are the self-discharge and charge-discharge efficiency coefficients. Constraint (20) describes the state of charge dynamics due to charge and discharge. Constraint (21) determines that the final state of charge is equal to the initial state of charge in one day. Constraints (22)-(24) define the range of state of charge, charging power and discharging power of the ES, respectively.

The power limit constraints are,

$$0 \le P_{\mathrm{pv}}^{t} \le P_{\mathrm{pv,f}}^{t}, \forall t \tag{25}$$

$$0 \le P_{\mathrm{wt}}^{t} \le P_{\mathrm{wt,f}}^{t}, \forall t \tag{26}$$

$$0 \le P_{\mathrm{b}}^{t} \le S_{\mathrm{vsc,max}}, \forall t \tag{27}$$

$$0 \le P_{\mathrm{s}}^{t} \le S_{\mathrm{vsc,max}}, \forall t \tag{28}$$

Note that only active power limit of the VSC needs to be considered in constraints (27)-(28) so that the MG model is a linear model. Reactive power is dispatched by the ADN and the full capacity constraint has been considered in (13).

The ADN optimization model (1)-(4), (8)-(17) and MG optimization model (18)-(28) constitute a Stackelberg game problem. The distributed iteration method [19] and unified solving method [28] can be used to solve this kind of problem. However, the day-ahead Stackelberg game model proposed in this paper has multiple Nash equilibrium solutions due to the time-of-use price mechanism. The distributed iteration method cannot guarantee the optimality of the Nash equilibrium solution. Therefore, the unified solving method is adopted. By using the Karush-Kuhn-Tucker (KKT) condition and strong duality theory, the Stackelberg game model can be transformed into a mixed integer second-order conic programming (MI-SOCP) problem to be efficiently solved. Due to limited space, the detailed transformation process is omitted and can be seen in [28].

4. Day-ahead reactive power optimization model

The day-ahead game model determines the time-of-use price, the active power exchange plan for each MG and minimum operation cost of the ADN satisfying the Nash equilibrium. But the voltage quality has not been considered. Therefore, the reactive power optimization model is conducted to fully utilize the residual capacity of VSCs and minimize system voltage deviation with the tolerant operation cost constraint. Since the adjustment of reactive power does not change the internal scheduling scheme of MGs, the constraints of MGs can be omitted in this model to improve the solving efficiency.

The objective of the reactive power optimization model is to minimize system voltage deviation:

$$\min \sum_{t=1}^{n} \sum_{\forall j \in B} (V_j^t - 1)^2 \tag{29}$$

The tolerant operation cost constraint is,

$$\sum_{t=1}^{n} \left[\begin{array}{l} \sum_{m=1}^{z_1} C_{\mathrm{e}}^{t} P_{\mathrm{e},m}^{t} + \sum_{m=1}^{z_2} (C_{\mathrm{d,base}} + C_{\mathrm{d,p}}) P_{\mathrm{d},m}^{t} \\ + \sum_{m=1}^{z_3} (C_{\mathrm{s},m}^{t} P_{\mathrm{s},m}^{t} - C_{\mathrm{b},m}^{t} P_{\mathrm{b},m}^{t}) \end{array} \right] \Delta t \le (1+\omega) L \tag{30}$$

where ω is the operation cost relaxation coefficient, and $C_{\mathrm{b},m}^{t}, C_{\mathrm{s},m}^{t}, P_{\mathrm{b},m}^{t}, P_{\mathrm{s},m}^{t}, L$ are fixed parameters obtained from the Stackelberg game model.

The rest constraints are the same as (2)-(13).

5. Intraday droop control dispatch model

The intraday dispatch is conducted in each day-ahead time step. Based on short-term forecast data, the day-ahead dispatch interval Δt is further divided into N intraday dispatch intervals, i.e., $\Delta t = N\Delta\tau$. In the intraday dispatch stage, in order to mitigate the impact of the uncertain power exchange between the ADN and MGs, $V^2 - P$ and $V^2 - Q$ dual droop control are implemented in the multiple terminal SOP. Then, the robust optimization model of droop parameters is established to minimize total network losses of the ADN under expected scenarios while ensuring the system robust security within the RES uncertainty set.

The uncertainty of RESs inside MGs can be represented as the uncertainty of net active power exchange between the ADN and MGs equivalently, as shown in (31).

$$U = \left\{ P_{\mathrm{vsc},m} \left| \begin{array}{l} u_{\min,m} \le P_{\mathrm{vsc},m} \le u_{\max,m}, \forall m \\ u_{\min,m} = P_{\mathrm{vsc},m}^{\mathrm{f}} - \theta P_{\mathrm{res},m}^{\mathrm{f}}, u_{\max,m} = P_{\mathrm{vsc},m}^{\mathrm{f}} + \theta P_{\mathrm{res},m}^{\mathrm{f}} \end{array} \right. \right\} \tag{31}$$

where U represents the uncertainty set, θ is the forecast error, and $P_{\mathrm{vsc},m}^{\mathrm{f}}$ and $P_{\mathrm{res},m}^{\mathrm{f}}$ are day-ahead active power exchange and the forecast total RES output power of the m^{th} MG.

Take $\boldsymbol{y}$ as the intraday system state vector, $\boldsymbol{k}$ as the slope vector and $\boldsymbol{D}$ as the expected scenario set. Then according to the CCG algorithm, the intraday model can be decomposed into a master problem (MP), i.e., the slope optimization model and a subproblem (SP), i.e., the extreme scenario optimization model. The MP is to optimize the slopes that can minimize the total network losses and guarantee the system security under limited extreme scenarios found by the SP. While the SP is to identify the scenario where the security constraints are violated most seriously under the given slopes, and collect this scenario into the extreme scenario set. The MP is shown in (32)-(37).

$$\text{(MP)} \qquad \min_{\boldsymbol{k}} \sum_{\tau=1}^{N} \sum_{m=1}^{z_1} P_{\mathrm{e},m}^{\tau} \tag{32}$$

$$\forall P_{\mathrm{e},m}^{\tau} \in K^{l} \text{ and } \forall P_{\mathrm{e},m}^{\tau} \in D, \exists \boldsymbol{y}, \text{ such that}$$

$$s.t. \ (2)-(5), (9)-(13) \tag{33}$$

$$V_{\mathrm{ref},i}^{2} - \tilde{V}_{i}^{\tau} = k_{\mathrm{p},i}(P_{\mathrm{sop},i}^{\tau} - P_{\mathrm{ref},i}), \forall \tau, \forall i \in B_{\mathrm{sop,S}} \tag{34}$$

$$V_{\mathrm{ref},i}^{2} - \tilde{V}_{i}^{\tau} = k_{\mathrm{q},i}(Q_{\mathrm{sop},i}^{\tau} - Q_{\mathrm{ref},i}), \forall \tau, \forall i \in B_{\mathrm{sop,S}} \cup B_{\mathrm{sop,M}} \tag{35}$$

$$k_{\min} \le k_{p,i} \le k_{\max} \tag{36}$$

$$k_{\min} \le k_{q,i} \le k_{\max} \tag{37}$$

where $V_{\text{ref},i}, P_{\text{ref},i}, Q_{\text{ref},i}$ are the droop reference values obtained by the day-ahead model. Constraints (34)-(35) are droop equations. The multiple terminals of the SOP can share the intraday power fluctuations through flexible power regulation based on the optimal droop curves. Constraints (36)-(37) define the range of droop slopes. Note that one of the terminals should be chosen as the master terminal to maintain the DC voltage of the SOP [29].

The SP is shown in (38)-(41).

$$(SP)\quad \eta^l = \max_{\boldsymbol{P}_{\text{vsc},m}} \min_{\boldsymbol{y},\boldsymbol{s}^{\text{u}},\boldsymbol{s}^{\text{d}}} (1^{\text{T}}\boldsymbol{s}_{\text{u}} + 1^{\text{T}}\boldsymbol{s}_{\text{d}} + 1^{\text{T}}\boldsymbol{s}_{\text{c}}) \tag{38}$$

$$s.t.\ (2)-(4),\ (8),\ (11)-(13),\ (34)-(35) \tag{39}$$

$$V_{\min}^2 \le \tilde{V}_i + s_{\text{u},i} - s_{\text{d},i} \le V_{\max}^2, \forall i \in B \tag{40}$$

$$0 \le \tilde{I}_{ij} - s_{\text{c},ij} \le I_{\max}^2, \forall (i,j) \in E \tag{41}$$

where $\boldsymbol{s}_{\text{u}} = [s_{\text{u},1}, s_{\text{u},2}, ..., s_{\text{u},i}, ..., s_{\text{u},N}]^{\text{T}}$, $\boldsymbol{s}_{\text{d}} = [s_{\text{d},1}, s_{\text{d},2}, ..., s_{\text{d},i}, ..., s_{\text{d},N}]^{\text{T}}$ and $\boldsymbol{s}_{\text{c}} = [s_{\text{c},1}, s_{\text{c},2}, ..., s_{\text{c},ij}, ..., s_{\text{c},M}]^{\text{T}}$. $s_{\text{u},i}$, $s_{\text{d},i}$ and $s_{\text{c},ij}$ are defined as non-negative relaxation variables to evaluate the security constraint violation. Therefore, the security constraints (9)-(10) can be relaxed into (39)-(40). If the objective function η^l in the SP equals zero, the droop parameters obtained by the MP will be robust within the uncertainty set.

The objective function of the SP is to minimize the sum of the security constraint relaxation variables, which is not a strictly increasing function of the branch current. Under this circumstance, the SOC relaxation may be inaccurate and influence the reliability of the dispatch commands [24]. Therefore, to solve this problem, a branch loss limit strategy is proposed. By pre-evaluating the maximum loss of each branch, extra inequality constraints (42) are added in the SP to restrain the feasible range of branch current and reduce the SOC relaxation gap:

$$r_{ij}\tilde{I}_{ij} \le \varepsilon_{ij}, \forall (i,j) \in E \tag{42}$$

where ε_{ij} is defined as the maximum branch loss under the given slopes, which is obtained by solving the following problems:

$$\begin{aligned} \varepsilon_{ij} &= \max_{P_{\text{vsc},m} \in U} r_{ij}\tilde{I}_{ij}, \forall (i,j) \in E \\ &s.t.\ (2)-(4), (8)-(13), (34)-(35) \end{aligned} \tag{43}$$

The principle of the proposed branch loss limit strategy is that when SOC relaxation is inaccurate, part of the branch current will falsely increase into the infeasible region to minimize the objective that is not positively related to the current. Therefore, by adding a series of current inequality constraints, the current violation can be effectively suppressed.

Then according to the duality theory, the above SP model (38)-(42) can be further transformed into a single-level MI-SOCP problem to be efficiently solved. The specific transformation process can be seen in [23].

The overall solving process of the intraday robust dispatch model is shown in Fig. 3.

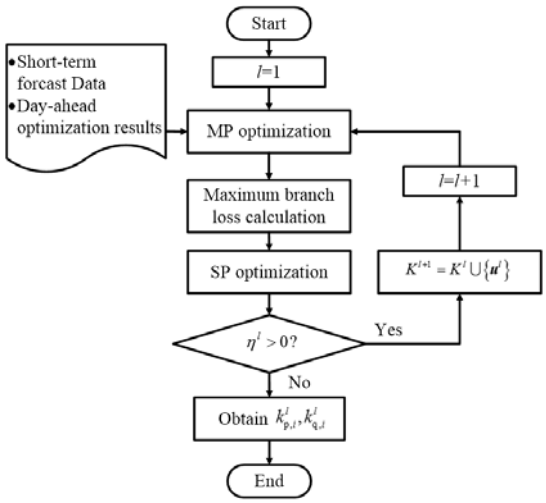

Fig. 3. The overall solving process of the intraday dispatch model.

6. Case study

The ADN used to test the proposed method is shown in Fig. 4. By modifying IEEE 37-bus, IEEE 13-bus and IEEE 34-bus standard test systems, three AC subgrids AC_A, AC_B and AC_C are connected by a five-terminal SOP. The modular multilevel converter (MMC) is applied in each terminal of the SOP. T_A, T_B and T_C are 110/10kV transformers, which are responsible for maintaining the voltage and frequency of slack buses. MMC1 is the master terminal, and the remaining MMCs are slave terminals. The voltage feasible range is set to $1 \pm 7\%$ (p.u.). Seven MGs MG1-MG7 are connected to the buses 9, 14, 18, 30, 37, 47, 59, respectively. The system parameters are modified from [18]. The number of day-ahead dispatch periods $n = 24$, and the time interval $\Delta t = 1$h. The number of intraday dispatch periods $N = 4$, and the time interval $\Delta\tau = 15$ min. The day-ahead Stackelberg game model and the intraday SP model are MI-SOCP models, solved by the Gurobi 7.0.2 solver with MATLAB 2014b, and the single solving time is about 140 secs and 27 secs, respectively. The reactive power re-optimization model and the intraday MP model are nonlinear models, solved by the CONOPT solver with GAMS 23.8, and the single solving time is about 170 secs and 1.4 secs, respectively. The data in the case study are represented by per-unit values.

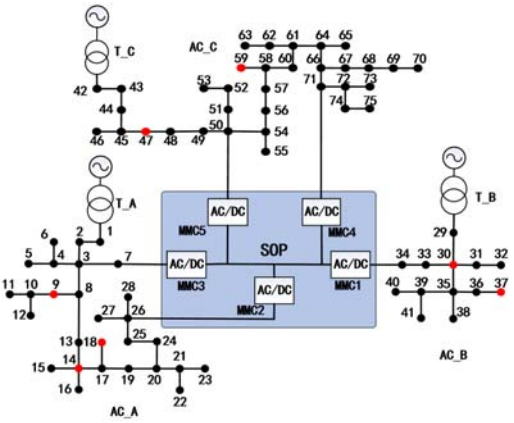

Fig. 4. The SOP-based ADN topology.

6.1. Day-ahead economic analysis of active distribution network

To demonstrate the advantages of the proposed time-of-use

price game model, five methods are used to conduct the day-ahead game optimization. The results are shown in Table I.

Method (1): The SOP is deployed in the ADN, and the Stackelberg game model is solved by the unified solving method (The proposed energy management method).

Method (2): The SOP is deployed in the ADN. The time-of-use price mechanism is not adopted. The 24-hour selling and buying price are assumed to be the same respectively.

Method (3): The SOP is deployed in the ADN, and the Stackelberg game model is solved by the distributed iteration method [19].

Method (4): The SOP is deployed in the ADN. Assume that MGs don't participate in the Stackelberg game, and can be fully dispatched by the ADN. The ADN trades electricity with MGs based on the time-of-use price of the main grid.

Method (5): The SOP is not deployed in the ADN. Three subgrids are optimized independently by the proposed energy management method.

TABLE I
COMPARISONS OF ECONOMIC EFFICIENCY OF DIFFERENT METHODS

	Operation cost of ADN	Operation cost of MGs	Average selling price	Average buying price	Selling electricity	Buying electricity	DG generation
(1)	320243	28705	3246.8	7472.6	8.673	6.386	0
(2)	323251	51278	1500.0	15000	5.686	3.398	0.322
(3)	348283	28875	2687.6	8062.5	5.686	3.407	0.446
(4)	305230	43692	2687.6	8062.5	8.442	6.156	0
(5)	566963	28433	3075.9	7357.9	8.347	6.060	5.570

By comparing *Method (2)* with *Method (1)*, it can be seen that when fixed price mechanism is adopted, the optimal selling price is always at the lower limit, and the optimal buying price is always at the upper limit. MGs cannot gain any profit from electricity trading process, thus they have no enthusiasm to participate in the power interaction, and only passively trade electricity with the ADN when the ES is full or empty to keep power balance. Therefore, both selling and buying electricity in *Method (2)* are significantly less than that of *Method (1)*. In addition, the total generation power of controllable DGs is 0.322 in *Method (2)*, which indicates that the power exchange plan formulated by MGs cannot guarantee power balance and steady-state security of the ADN. While in *Method (1)*, through the optimal adjustment of time-of-use price, MGs can use the ES to provide peak shaving and valley filling to increase their own profit as well as improve the power flow security and operation economy of the ADN. Therefore, the total generation power of controllable DGs is 0, and the operation cost of both the ADN and MGs are less than that of *Method (2)*.

By comparing *Method (3)* with *Method (1)*, it can be seen that the time-of-use price model has multiple Nash equilibrium solutions. For any given power exchange plan, the ADN will charge at the boundary of the time-of-use selling and buying price limit, thus the distributed iteration method cannot guarantee the optimality of the Nash equilibrium solution. As a result, the price optimization is invalid with higher operation cost of both the ADN and MGs, and the final power exchange plan of MGs is similar than that of *Method (2)*.

By comparing *Method (4)* with *Method (1)*, it can be seen that when MGs can be fully dispatched by the ADN, the power flow controllability of the ADN is enhanced, thus the operation economy and security of the ADN are significantly improved. The ADN operation cost is reduced to 305230 without activating controllable DGs. However, the unified dispatch scheme greatly sacrifices the economic interests of MG owners. The total operation cost of MGs increases from 28705 to 43692 with the increasing rate about 52.2%. The large reduction of economic benefits of MGs is not conducive to the benign development of the ADN power market.

By comparing *Method (5)* with *Method (1)*, it can be seen that the SOP plays a significant role in power flow regulation of the ADN. In *Method (5)*, since three subgrids are independent of each other, they lack the ability to adjust power flow direction and realize emergency power support. At this time, by adjusting the time-of-use price, the ADN further encourages MGs to participate in the power flow regulation to earn more profit. Therefore, the total operation cost of MGs is lower than that of *Method (1)*. Besides, without the SOP, due to the current restriction of the branches, the rest power shortage can only be met by controllable DGs. Therefore, the total generation power of controllable DGs in *Method (5)* is 5.570. Considering the penalty cost, the total operation cost of the ADN is remarkably increased to 566963.

Through the above analysis, it can be concluded that the SOP can realize flexible power flow regulation and mutual power support among multiple subgrids. The proposed Stackelberg game can effectively optimize the time-of-use price to guild MGs to make more reasonable power exchange plan to guarantee the economic benefits of MG owners while improving the ADN power flow.

6.2. Day-ahead economic analysis of microgrids

Take MG1, MG2 and MG3 in the subgrid AC_A as examples. Assume they have the same internal parameters and day-ahead forecast data. In the results of *Method (1)*, the time-of-use price, VSC power exchange and the state of charge of the ES of these three MGs are shown in Figs. 5 - 8, respectively. The positive power direction is from the ADN to the MG.

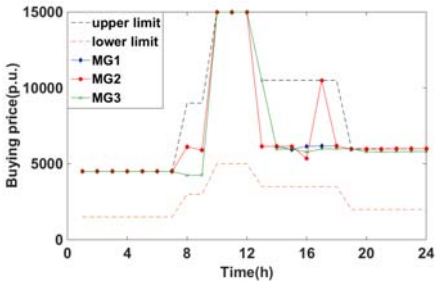

Fig. 5 Buying price of MGs.

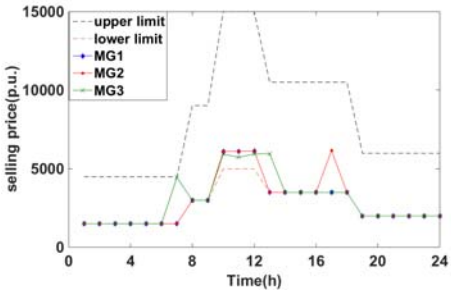

Fig. 6 Selling price of MGs.

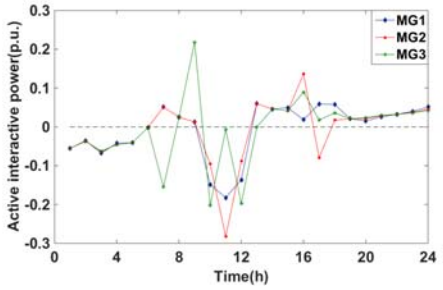

Fig. 7 Active power exchange of VSCs.

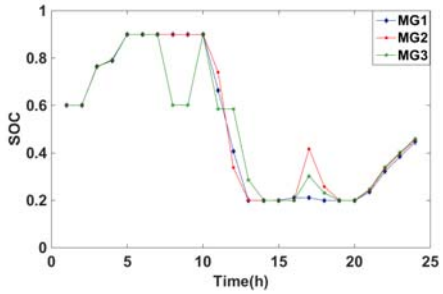

Fig. 8 The SOC of the ES.

As shown in Figs. 5 and 6, due to the difference of grid-connected locations, the influence of VSC power exchange of each MG on the power flow is also different. Therefore, different prices are made for MGs. Besides, the optimal buying and selling prices in the single MG are different too, which indicates that the independent optimization of buying and selling price has a better price incentive effect and can effectively reduce the operation cost of the ADN.

Take MG2 as an example. In 1-5 h, there is extra electricity in MG2, so the ES charges, and the rest excessive electricity can only be sold to the ADN. Therefore, the selling price is at its lower limit. In 10-12 h, the load of the ADN is heavy, therefore the selling price is increased above the lower limit to encourage the ES of MG2 to discharge and sell the electricity to the ADN. In 13-24 h, MG2 needs to buy electricity from the ADN to satisfy its own load demand. However, at 17 h, the ADN cannot sell electricity to MG2 due to power flow constraints, therefore both selling and buying price at this point are obviously increased, and the buying price of 16 h is decreased. In response to the price, the amount of electricity bought from the ADN is increased at 16 h and stored in the ES, then the ES discharges at 17 h to satisfy the load demand and sell extra electricity to the ADN to obtain arbitrage. The ADN can also benefit from the power flow improvement.

Based on the above discussions, it can be concluded that the proposed game model can adjust the time-of-use price flexibly to guide each MG to maximize its own benefit while providing peak shaving and valley filling to the ADN.

6.3. Pareto front of reactive power optimization model

The day-ahead game model only takes economic efficiency into account, thus the voltage profile of the ADN will be close to the upper bound to minimize the network loss, which may increase the risk of voltage security constraint violation in real time operation. Therefore, the reactive power optimization is conducted to minimize the voltage deviation of the ADN with the tolerant cost constraint to keep a balance between economic efficiency and voltage safety of the ADN. By adjusting the cost relaxation coefficient, the Pareto front of the operation cost and voltage deviation is shown in Fig. 9.

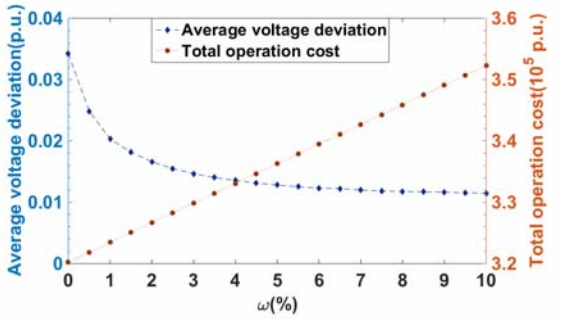

Fig. 9 The Pareto front of the operation cost and voltage deviation.

As shown in Fig. 9, with the increase of cost relaxation coefficient ω, the total operation cost increases linearly, while the average voltage deviation decreases fast at first, and then gradually decreases due to the limit of power flow constraints. $\omega = 2\%$ is chosen in this paper, and with the increase of only 2% of the total ADN operation cost, the average voltage deviation can be decreased from 0.034 to 0.016 by 53%. Therefore, the reactive power optimization can fully utilize the residual capacity of VSCs to provide reactive power support and improve the voltage quality at a small economic cost.

6.4. Security analysis in intraday dispatch

During the intraday dispatch, the actual output power of RESs may deviate from the forecast data, which will lead to fluctuations of the power exchange between the ADN and MGs and may risk the safety of the system. In order to analyze the intraday system security performance, take one period with high PV generation as an example. Based on the day-ahead reference point and short-term forecast data, the droop slopes are optimized under different forecast errors by the following two methods respectively.

Method (6): The proposed robust optimization method.

Method (7): The deterministic slope optimization, which only considers safe operation under the expected scenarios.

For each forecast error, 1000 test scenarios are randomly generated in the uncertainty set to examine the optimized droop commands. The results are shown in Table II. The reliable probability index (RPI) are designed to reflect the system security performance:

$$\mathrm{RPI} = \frac{N_{\mathrm{secure}}}{N_{\mathrm{sample}}} \tag{44}$$

where N_{sample} is the total sampling number, and N_{secure} is the number of secure samples which satisfy voltage and power flow constraints.

TABLE II
SECURITY ANALYSIS IN THE INTRADAY DISPATCH

θ	Average network loss		RPI under test scenarios	
	(6)	*(7)*	*(6)*	*(7)*
5%	0.1043	0.0983	100%	94.6%
10%	0.1086	0.0983	100%	89.2%
15%	0.1117	0.0983	100%	80.9%
20%	infeasible	0.0983	infeasible	76.1%

As shown in Table II, since the influence of random fluctuations of RESs is not considered in *Method (7)*, the average network loss under expected scenarios remains the same at 0.0983. However, with the increase of forecast errors, the RPI under the test scenarios decreases gradually. By comparison, the results of *Method (6)* tend to be more conservative in order to deal with greater uncertainty. With the

increase of θ from 5% to 15%, the average network under expected scenarios increases, but the system security can be guaranteed under all test scenarios. Therefore, the system security has been greatly improved by robust optimization at the expense of a small economic cost. Besides, when θ is further increased to 20%, *Method (6)* is infeasible, which indicates that the RES fluctuations are too large. With $\theta = 20\%$, the system cannot deal with all uncertainty only by droop parameter optimization, and additional load reduction or PV limit strategies are needed, which will be our next research goal.

To further test the effectiveness of the robust droop control method during different time periods, assume that the intraday forecast error $\theta = 10\%$, and take 24 dispatch intervals in each hour during all day operation as an example. *Method (8)* is adopted in the intraday operation and compared with *Method (6)*.

Method (8): $P-Q$ control is adopted in the slave terminals of the SOP, following the day-ahead dispatch commands. While $V_{dc}-Q$ control is adopted in the master terminal to maintain the DC voltage of the SOP.

1000 test scenarios are randomly generated in each dispatch interval to examine the all day performance of these two methods. The RPI and average network loss comparison results are shown in Fig. 10 and Fig. 11 respectively.

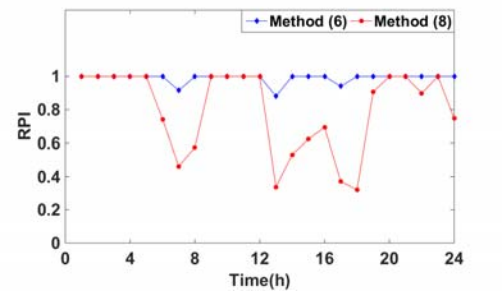

Fig. 10 The RPI statistical results.

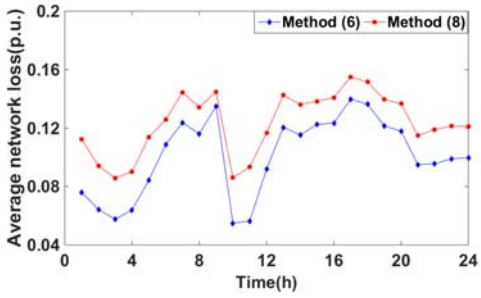

Fig. 11 The average network loss statistical results.

As shown in Fig. 9, compared with the traditional *P-Q* control, the proposed robust droop control method can effectively improve the system adaptability to the intraday RES power fluctuations. The average RPI during all day operation is increased from 80.1% to 98.9%. Note that in *Method (6)*, at *t*=7 h, 13 h and 17 h, the day-ahead optimal reference operation points are close to the steady-state safety boundary, thus the intraday slope robust optimization is infeasible, and system security can only be guaranteed in the expected scenarios. Therefore, in these three dispatch intervals, there is still a probability of violating system security constraints, and RPI is less than 1.

As shown in Fig. 10, during all day operation, the network loss of *Method (6)* is always lower than that of *Method (8)*. The total average network loss is reduced from 0.1233 to 0.1008. The reason is that when P-Q control is adopted, the power fluctuations at the end of the ADN are ultimately absorbed by the upper grid. Long distance power transmission will increase the network loss. While the droop control can achieve power complementation among different subgrids to effectively reduce total unbalanced power. Besides, it can be seen that in 10-12 h, the network loss of both methods decreases significantly. The reason is that during day-ahead dispatch stage, through price optimization, MGs are encouraged to sell electricity to the ADN, thus long distance transmission power is reduced.

Through the above analysis, it can be concluded that the multiple terminals of the SOP can share the intraday power fluctuations through flexible power regulation based on the optimal droop curves to effectively improve system security and reduce network loss.

6.5. Validity of the branch loss limit strategy

To illustrate the validity of the proposed branch loss limit strategy, *Method (9)* is adopted to optimize the droop parameters and compared with *Method (6)*. The results are shown in Table III. The maximum SOC relaxation gap is defined as follows to measure the inaccuracy of the SOC relaxation quantitatively:

$$\Delta_{\max} = \max\{I_{ij}^2 V_i^2 - (P_{ij}^2 + Q_{ij}^2), \forall (i,j) \in E\} \tag{45}$$

where $\Delta_{\max}$ is the maximum deviation of the right hand side of (5) minus the left hand side.

Method (9): The robust optimization without considering the branch loss limit strategy, which means the inequality sets (42) are not included in the SP model.

TABLE III
VALIDITY OF THE BRANCH LOSS LIMIT STRATEGY

θ	*(6)*			*(9)*		
	RPI	$\Delta_{\max}$	Iterations	RPI	$\Delta_{\max}$	Iterations
5%	100%	0.3863	3	95.1%	1.6311	2
10%	100%	0.4121	4	92.7%	1.7142	2
15%	100%	0.4626	4	84.7%	1.8939	3

As shown in Table III, in *Method (9)*, when the relaxation gap is too large, part of the branch current will falsely increase into the infeasible region to minimize the voltage relaxation variables that are not positively related to the current, therefore part of the extreme scenarios cannot be found accurately by the SP model, and RPI decreases gradually with the increase of forecast errors. While *Method (6)* can effectively reduce the maximum relaxation gap and improve the searching ability of SP for the extreme scenarios by adding the current limit constraints. Therefore, more extreme scenarios can be identified, and the probability of security constraint violation can remain at zero, which improves the system robust security. Note that the proposed method cannot completely eliminate the inaccuracy of the second-order cone relaxation gap, but small relaxation gap is acceptable in this paper since the goal of the SP model is only to find the extreme scenarios. The accurate power flow results in the extreme scenario will be recalculated in the MP model.

7. Conclusions

This paper proposes a multi-time scale robust energy management method for the SOP based ADN considering game

relationship between the ADN and MGs. In the day-ahead dispatch, a Stackelberg pricing game model is established to balance the economic benefit of the ADN and each MG under power flow constraints. Then a reactive power re-optimization model is established to make a trade-off between economic efficiency and voltage deviation of the ADN with the tolerant cost constraint. In the intraday dispatch, $V^2 - P$ and $V^2 - Q$ dual droop control mode is implemented in the SOP, and a slope robust optimization model is established to improve system robust security in face of output uncertainty of RESs. Numerical experiments show that:

1) The proposed Stackelberg game model can adjust the time-of-use price flexibly to motivate MGs to provide peak shaving and valley filling to the ADN on the premise of guaranteeing economic benefits of all participants.

2) The proposed reactive power re-optimization model can fully utilize the residual capacity of VSCs to decrease ADN voltage deviation at a small adjustable economic cost.

3) The intraday slope robust optimization model can guarantee system security within a certain range of RES output uncertainty, and the proposed branch loss limit strategy can reduce the maximum SOC relaxation gap in the SP model to improve the reliability of the slope optimization results.

REFERENCES

[1] T. Xu, W. Wu, W. Zheng et al., "Fully Distributed Quasi-Newton Multi-Area Dynamic Economic Dispatch Method for Active Distribution Networks," *IEEE Trans. Power Syst.*, vol. 33, no. 4, pp. 4253-4263, Jul. 2018.

[2] P. Li, H. Ji, C. Wang et al., "Optimal Operation of Soft Open Points in Active Distribution Networks Under Three-Phase Unbalanced Conditions," *IEEE Trans. Smart Grid*, vol. 10, no. 1, pp. 380-391, Jan. 2019.

[3] W. Cao, J.Wu, and N.Jenkins, "Operating principle of soft open points for electrical distribution network operation," *Appl Energ*, vol. 164, pp. 245–257, 2016.

[4] J. M. Bloemink and T. C. Green, "Benefits of Distribution-Level Power Electronics for Supporting Distributed Generation Growth," *IEEE Trans. Power Deliv*, vol. 28, no. 2, pp. 911-919, Apr. 2013.

[5] P. Li, H. Ji, C. Wang et al., "Coordinated Control Method of Voltage and Reactive Power for Active Distribution Networks Based on Soft Open Point," *IEEE Trans. Sustain. Energy*, vol. 8, no. 4, pp. 1430-1442, Oct. 2017.

[6] B. Zhao, M Xue, X Zhang et al., "An MAS based energy management system for a stand-alone microgrid at high altitude," *Appl Energ*, vol. 143, pp. 251-261, 2015.

[7] W. Cao, J. Wu, and N. Jenkins, "Benefits analysis of soft open points for electrical distribution network operation," *Appl Energ*, vol. 165, pp. 36-47, 2016.

[8] Z. Wang, B. Chen, J. Wang et al., "Decentralized Energy Management System for Networked Microgrids in Grid-Connected and Islanded Modes," *IEEE Trans. Smart Grid*, vol. 7, no. 2, pp. 1097-1105, Mar. 2016.

[9] T. Morstyn, A. Teytelboym, and M. D. McCulloch, "Bilateral contract networks for peer-to-peer energy trading," *IEEE Trans. Smart Grid*, vol. 10, no. 2, pp. 2026–2035, Mar. 2019.

[10] S. Cui, Y. Wang, Y. Shi et al., "A New and Fair Peer-to-Peer Energy Sharing Framework for Energy Buildings," *IEEE Trans. Smart Grid*, vol. 11, no. 5, pp. 3817-3826, Sept. 2020.

[11] T. Chen and W. Su, "Indirect Customer-to-Customer Energy Trading With Reinforcement Learning," *IEEE Trans. Smart Grid*,, vol. 10, no. 4, pp. 4338-4348, July 2019.

[12] S. Cui, Y. Wang, J. Xiao et al., "A Two-Stage Robust Energy Sharing Management for Prosumer Microgrid," *IEEE Trans. Industr. Inform*, vol. 15, no. 5, pp. 2741-2752, May 2019.

[13] M. R. Sandgani and S. Sirouspour, "Priority-Based Microgrid Energy Management in a Network Environment," *IEEE Trans. Sustain. Energy*, vol. 9, no. 2, pp. 980-990, Apr. 2018.

[14] Z. Wang, B. Chen, J. Wang et al., "Coordinated Energy Management of Networked Microgrids in Distribution Systems," *IEEE Trans. Smart Grid*, vol. 6, no. 1, pp. 45-53, Jan. 2015.

[15] A. P. Mazzini, E. N. Asada and G. G. Lage, "Minimisation of active power losses and number of control adjustments in the optimal reactive dispatch problem," *IET Gener Transm Dis*, vol. 12, no. 12, pp. 2897-2904, Oct. 2018.

[16] N. G. Paterakis, A Mazza, S. F. Santos et al., "Multi-Objective Reconfiguration of Radial Distribution Systems Using Reliability Indices," *IEEE Trans. Power Syst.*, vol. 31, no. 2, pp. 1048-1062, Mar. 2016.

[17] E. Ela and M. O'Malley, "Studying the Variability and Uncertainty Impacts of Variable Generation at Multiple Timescales," *IEEE Trans. Power Syst.*, vol. 27, no. 3, pp. 1324-1333, Aug. 2012.

[18] F. Sun, J. Ma, M. Yu *et al.*, "A Robust Optimal Coordinated Droop Control Method for Multiple VSCs in AC–DC Distribution Network," *IEEE Trans. Power Syst.*, vol. 34, no. 6, pp. 5002-5011, Nov. 2019.

[19] Y. Liu, L. Guo and C. Wang, "A robust operation-based scheduling optimization for smart distribution networks with multi-microgrids," *Appl Energ*, vol. 228, pp. 130-140, 2018.

[20] H. Ji, C. Wang, P. Li et al., "Robust Operation of Soft Open Points in Active Distribution Networks With High Penetration of Photovoltaic Integration," *IEEE Trans. Sustain. Energy*, vol. 10, no. 1, pp. 280-289, Jan. 2019.

[21] W. Wei, F. Liu, S. Mei et al., "Robust Energy and Reserve Dispatch Under Variable Renewable Generation," *IEEE Trans. Smart Grid*, vol. 6, no. 1, pp. 369-380, Jan. 2015.

[22] B. Zhao, X. Wang, D. Lin et al., "Energy Management of Multiple Microgrids Based on a System of Systems Architecture," *IEEE Trans. Power Syst.*, vol. 33, no. 6, pp. 6410-6421, Nov. 2018.

[23] T. Ding, C. Li, Y. Yang et al., "A Two-Stage Robust Optimization for Centralized-Optimal Dispatch of Photovoltaic Inverters in Active Distribution Networks," *IEEE Trans. Sustain. Energy*, vol. 8, no. 2, pp. 744-754, Apr. 2017.

[24] H. Gao, J. Liu and L. Wang, "Robust Coordinated Optimization of Active and Reactive Power in Active Distribution Systems," *IEEE Trans. Smart Grid*, vol. 9, no. 5, pp. 4436-4447, Sept. 2018.

[25] B. Zhao, H. Qiu, R. Qin et al., "Robust Optimal Dispatch of AC/DC Hybrid Microgrids Considering Generation and Load Uncertainties and Energy Storage Loss," *IEEE Trans. Power Syst.*, vol. 33, no. 6, pp. 5945-5957, Nov. 2018.

[26] Z. Yang, H. Zhong, Q. Xia et al., "A Structural Transmission Cost Allocation Scheme Based on Capacity Usage Identification," *IEEE Trans. Power Syst.*, vol. 31, no. 4, pp. 2876-2884, Jul. 2016.

[27] D. Wang, S. Ge, H. Jia et al., "A Demand Response and Battery Storage Coordination Algorithm for Providing Microgrid Tie-Line Smoothing Services," *IEEE Trans. Sustain. Energy*, vol. 5, no. 2, pp. 476-486, Apr. 2014.

[28] W. Wei, F. Liu and S. Mei, "Energy Pricing and Dispatch for Smart Grid Retailers Under Demand Response and Market Price Uncertainty," *IEEE Trans. Smart Grid*, vol. 6, no. 3, pp. 1364-1374, May. 2015.

[29] J. Ma, G. Geng and Q. Jiang, "Two-Time-Scale Coordinated Energy Management for Medium-Voltage DC Systems," *IEEE Trans. Power Syst.*, vol. 31, no. 5, pp. 3971-3983, Sept. 2016.